pH Control of Photoreactivity of Ru(II) Pyridyltriazole Complexes: Photoinduced Linkage Isomerism and Photoanation

R. Wang,[†] J. G. Vos,*[,†] R. H. Schmehl,*[,‡] and R. Hage[§]

Contribution from the School of Chemical Sciences, Dublin City University, Dublin 9, Ireland, Department of Chemistry, Tulane University, New Orleans, Louisiana 70118, and Unilever Research Laboratory, Olivier van Noortlaan 120, 3133 AT Vlaardingen, The Netherlands.
Received August 19, 1991

Abstract: The photophysical and photochemical behavior of mixed ligand complexes of Ru(II) with 3-(pyridin-2-yl)-1,2,4-triazole (HPTN) have been examined in solutions of varying acidity. Protonation of both the N-2 bound (HPTN-2) and the N-4 bound (HPTN-4) isomers of $[(bpy)_2Ru(HPTN)]^+$ results in a decrease in the luminescence lifetime in solution and an increase in reactivity upon photolysis in CH_2Cl_2. The excited state of the deprotonated form of both complexes decays by a single exponential at pHs above 3; the data were fit to a general expression for excited-state decay involving protonation of the excited complex. Results of temperature-dependent luminescence decays suggest the protonated complexes decay via population of a metal-centered excited state, while the deprotonated complexes do not efficiently populate this state at temperatures at or below room temperature. Photolysis of either protonated isomer in CH_2Cl_2 results in linkage isomerism; equilibrium is established for photolysis at 4:1 $[(bpy)_2Ru(HPTN\text{-}4)]^{2+}$ to $[(bpy)_2Ru(HPTN\text{-}2)]^{2+}$. In the presence of coordinating counterions photoanation occurs to yield the cis-anion complex with loss of pyridyltriazole. The deprotonated form of both isomers is inert to photosubstitution in CH_2Cl_2 at room temperature. Thus, the substitutional photolability can be controlled by controlling protonation of the ground state of the complex.

Introduction

The photophysical behavior of numerous Ru(II) complexes having one or more diimine ligands has been the subject of numerous investigations.[1-4] For $[(bpy)_3Ru]^{2+}$ (bpy = 2,2'-bipyridine) relaxation of the emissive metal-to-ligand charge transfer (^{3}MLCT) state exhibits a temperature dependence in the 150–300 K range which has been ascribed to thermally activated population of a metal-centered excited state (^{3}MC) which decays more rapidly than the ^{3}MLCT state.[5] In nonaqueous solvents population of this ^{3}MC state results in labilization of one of the bipyridine ligands and subsequent decomposition of the complex, particularly in the presence of coordinating anions.[5-11] The relative energies of the ^{3}MLCT and ^{3}MC states can be controlled to some degree by making mixed ligand complexes in which there is a single weak σ donor diimine ligand with a relatively low π^* level and the remaining ligands are strong σ donors.[9-17] The result is to increase the ^{3}MLCT–^{3}MC splitting, thereby removing the thermally activated nonradiative decay path and inhibiting photoanation of the complex.

A wide body of literature exists demonstrating the effects of solution acidity on molecular luminescence. In general, excited states of photoactive acids have excited state pK_as which differ from those of the ground state. Further, the emission energies and nonradiative relaxation rates of protonated and dissociated forms differ. In metal diimine complexes two types of behavior exist for MLCT excited states having exchangeable protons.[17-27] In complexes where the lowest energy MLCT state involves charge transfer to the ligand exhibiting acid–base behavior, the excited state becomes more basic than the ground state. When the MLCT state is localized on another ligand, the pK_a decreases upon excitation of the complex. In all cases nonradiative decay of the complexes is strongly affected by protonation. Of fundamental importance is the rate of excited-state decay relative to proton exchange.[28] The kinetic scheme is summarized in SchemeI, where k_H and k_{-H} are the rate constants for protonation and deprotonation, of the excited complex, respectively, and k_{nr} is the sum of radiative and nonradiative decay rate constants of the excited complex. When proton exchange is much faster than excited-state decay of both free base and protonated complexes, a pseudo-

Scheme I

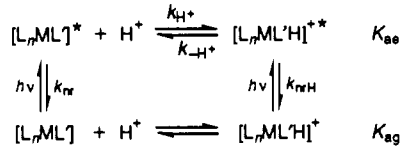

equilibrium exists in the excited state and the observed luminescence decay will be single exponential. In the opposite

[†] Dublin City University.
[‡] Tulane University.
[§] Unilever Research Laboratory.

(1) For a recent review see: Juris, F.; Balzani, V.; Barigelletti, F.; Campagna, S.; Belser, P.; von Zelewsky, A. *Coord. Chem. Rev.* **1988**, *82*, 85.
(2) Balzani, V.; Moggi, L.; Manfrin, F.; Bolletta, F.; Laurence, G. S. *Coord. Chem. Rev.* **1975**, *15*, 321.
(3) Kalyanasundaram, K. *Coord. Chem. Rev.* **1982**, *46*, 159.
(4) Meyer, T. J. *Pure Appl. Chem.* **1986**, *58*, 1193.
(5) (a) Van Houten, J.; Watts, R. J. *J. Am. Chem. Soc.* **1976**, *98*, 4853. (b) Van Houten, J.; Watts, R. J. *Inorg. Chem.* **1978**, *17*, 3381.
(6) (a) Hoggard, P. E.; Porter, G. B. *J. Am. Chem. Soc.* **1978**, *100*, 1457. (b) Wallace, P. E.; Hoggard, P. E. *Inorg. Chem.* **1980**, *19*, 2141.
(7) (a) Durham, B.; Walsh, J. C.; Carter, C. L.; Meyer, T. J. *Inorg. Chem.* **1980**, *19*, 860. (b) Durham, B.; Caspar, J. V.; Nagle, J. K.; Meyer, T. J. *J. Am. Chem. Soc.* **1982**, *104*, 4803. (c) Rillema, D. P.; Taghdiri, D. G.; Jones, D. S.; Keller, C. D.; Worl, L. A.; Meyer, T. J.; Levy, H. A. *Inorg. Chem.* **1987**, *26*, 578.
(8) (a) Pinnick, D. V.; Durham, B. *Inorg. Chem.* **1984**, *23*, 3841. (b) Pinnick, D. V.; Durham, B. *Inorg. Chem.* **1984**, *23*, 1440.
(9) (a) Wacholtz, W. F.; Auerbach, R. A.; Schmehl, R. H.; Ollino, M.; Cherry, W. R. *Inorg. Chem.* **1985**, *24*, 1758. (b) Wacholtz, W. F.; Auerbach, R. A.; Schmehl, R. H. *Inorg. Chem.* **1986**, *25*, 227.
(10) Henderson, T. J.; Cherry, W. R. *J. Photochem.* **1985**, *28*, 143.
(11) Kalyanasundaram, K. *J. Phys. Chem.* **1986**, *90*, 2285.
(12) (a) Allen, G. H.; White, R. P.; Rillema, D. P.; Meyer, T. J. *J. Am. Chem. Soc.* **1984**, *106*, 2613. (b) Barqawi, K. R.; Llobet, A.; Meyer, T. J. *J. Am. Chem. Soc.* **1988**, *110*, 7751. (c) Sullivan, B. P.; Salmon, D. J.; Meyer, T. J.; Peedin, J. *Inorg. Chem.* **1978**, *18*, 3369.
(13) Barigeletti, F.; Juris, F.; Balzani, V.; Belser, P.; von Zelewsky, A. *Inorg. Chem.* **1983**, *22*, 3335.
(14) (a) Haga, M.; Matsumur-Inoue, T.; Shimizu, K.; Sato, G. P. *J. Chem. Soc., Dalton Trans.* **1989**, 371. (b) Haga, M. *Inorg. Chim. Acta* **1983**, *75*, 29. (c) Haga, M.; Tsunemistsu, A. *Inorg. Chim. Acta* **1986**, *164*, 137. (d) Bond, A. M.; Haga, M. *Inorg. Chem.* **1986**, *25*, 4507. (e) Haga, M. *Inorg. Chim. Acta* **1980**, *45*, L183.
(15) (a) Steel, P. J.; Lahouse, F.; Lerner, D.; Marzin, C. *Inorg. Chem.* **1983**, *22*, 1488. (b) Marzin, C.; Budde, F.; Steel, P. J.; Lerner, D. *Nouv. J. Chim.* **1987**, *11*, 33. (c) Steel, P. J.; Constable, E. C. *J. Chem. Soc., Dalton Trans.* **1990**, 1389.
(16) Ross, H. B.; Boldaj, M.; Rillema, D. P.; Blanton, C. B.; White, R. P. *Inorg. Chem.* **1989**, *28*, 1013.

0002-7863/92/1514-1964$03.00/0

Table I. Room Temperature Photophysical Properties of Complexes Studied[a]

complex	solvent	λ_{max}, nm	λ_{em}, nm	ϕ_{em}	k_r, s^{-1}	τ_{em}^{298}, ns
$[(bpy)_2Ru(HPTN\text{-}4)]^{2+}$	$CH_3CN + CF_3COOH$	452	616	7.3×10^{-4}	2.8×10^4	2
$[(bpy)_2Ru(PTN\text{-}4)]^{+}$	$CH_3CN + Et_2NH$	484	678	6.3×10^{-3}	3.1×10^4	205
$[(bpy)_2Ru(HPTN\text{-}2)]^{2+}$	$CH_3CN + CF_3COOH$	442	611	4.3×10^{-4}	8.6×10^4	5
$[(bpy)_2Ru(PTN\text{-}2)]^{+}$	$CH_3CN + Et_2NH$	484	677	3.0×10^{-3}	2.1×10^4	142
$[(bpy)_3Ru]^{2+}$	CH_3CN	450	611	0.062[42]	6×10^4 [7b]	860[7b]

[a] Margins of error are λ_{max} ±2 nm, λ_{em} ±2 nm, ϕ_{em} ±20%, and τ_{em}^{298} ±10%.

Table II. Activation Parameters from Temperature-Dependent Luminescence Lifetimes in 4:1 EtOH/MeOH

complex	k_0, s^{-1}	k', s^{-1}	E_a, cm^{-1}	110 K τ_{em}, ns	298 K η_{ic}
$[(bpy)_2Ru(HPTN\text{-}4)]^{2+}$	6.1×10^6	9.2×10^{13}	2860	3548	0.94
$[(bpy)_2Ru(PTN\text{-}4)]^{+}$	1.6×10^6	3.1×10^7	600	1570	
$[(bpy)_2Ru(HPTN\text{-}2)]^{2+}$	1.6×10^6	6.0×10^{10}	1710	3635	0.91
$[(bpy)_2Ru(PTN\text{-}2)]^{+}$	1.7×10^6	4.7×10^7	550	2436	

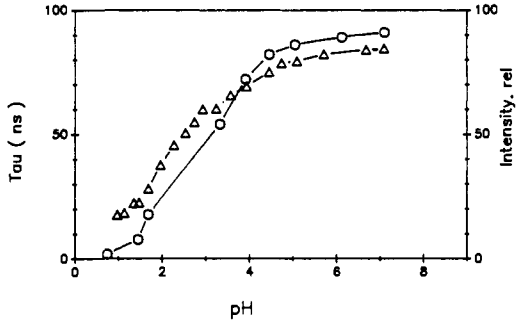

Figure 1. Relative luminescence intensity (△) and lifetime (○) of $[(bpy)_2Ru(PTN\text{-}2)]^{+}$ as a function of pH in Britton–Robinson buffer solutions at room temperature.

extreme the decay of the protonated and free base complexes is independent. Recently Scandola and co-workers have shown that the rate of acid dissociation of $[(bpy)_2Ru(CNH)(CN)]^{+}$ in pure CH_3CN is slow relative to the excited-state decay.[18] Further, the protonated complex has a much shorter lifetime than $[(bpy)_2Ru(CN)_2]$. As water is added to CH_3CN solutions of the complex, the rate of H^+ exchange increases until, at water concentrations >0.1 M, excited-state equilibration occurs faster than relaxation. The decrease in luminescence lifetime upon protonation was attributed to a new nonradiative decay path arising from a decrease in the MLCT/MC energy gap upon protonation. The acid base characteristics of unsymmetrical diimine ligands such as 3-(pyridin-2-yl)-1,2,4-triazole (HPTN) coordinated to Ru(II) have also been investigated.[17,29-34] The complexes are interesting because coordination to the Ru center can occur through either N-2 or N-4 of the triazole and the spectroscopic and redox characteristics of the resulting complexes depend not only on the mode of coordination but also on the protonation of the noncoordinated nitrogen.[29] Preliminary photophysical studies of the complexes $[(bpy)_2Ru(PTN\text{-}4)]^{+}$ and $[(bpy)_2Ru(PTN\text{-}2)]^{+}$ (and

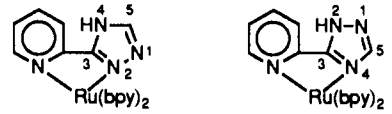

$[(bpy)_2Ru(HPTN\text{-}2)]^{2+}$ $[(bpy)_2Ru(HPTN\text{-}4)]^{2+}$

the protonated forms HPTN-2 and HPTN-4) showed that the luminescence lifetime of the deprotonated form of the complex is much longer than that of the protonated complex for both modes of coordination.[29,34] In this work, a more detailed analysis of the photophysics of the pyridyltriazole complexes above is presented. In addition, photoanation of the complexes was examined in both acidic and basic CH_2Cl_2, and evidence is presented for photoinduced linkage isomerization of the HPTN-4 to HPTN-2 complex (and vice versa) in CH_2Cl_2. Results from temperature-dependent luminescence lifetime and photosubstitution studies suggest that the relative energy difference between metal-centered and MLCT excited states is influenced by protonation of the noncoordinated nitrogen center and that the change in nonradiative relaxation upon protonation is the result of the change in the $^3MLCT/^3MC$ energy gap.

Results

The preparation, separation of isomers, and characterization of the complexes were presented in previous work.[17d,30,34,35] Metal-to-ligand charge-transfer absorption and luminescence maxima in room temperature acetonitrile are given in Table I. Spectra were taken in the presence of either a weak base (diethylamine) or an acid (trifluoroacetic acid) to generate either the free base or protonated forms of the complexes (see Experimental Section). Both absorption and emission spectra are very similar for the two isomers in aprotic solvents (CH_3CN, CH_2Cl_2), while significant differences (~10 nm) are observed between the maxima of the isomers in aqueous solutions.[35] Luminescence lifetimes and quantum yields relative to $[(bpy)_3Ru]^{2+}$ are also reported for the complexes in Table I. The striking observation is the large increase in the luminescence intensity and lifetime

(17) (a) Vos, J. G., Haasnoot, J. G.; Vos, G. *Inorg. Chim. Acta* **1983**, *71*, 155. (b) Hage, R.; Haasnoot, J. G.; Reedijk, J.; Wang, R.; Ryan, E.; Vos, J. G.; Spek, A. L.; Duisenberg, A. J. M. *Inorg. Chim. Acta* **1990**, *174*, 77. (c) Buchanan, B. E.; Wang, R.; Vos, J. G.; Hage, R.; Haasnoot, J. G.; Reedijk, J. *Inorg. Chem.* **1990**, *29*, 3263. (d) Long, C. J.; Vos, J. G. *Inorg. Chim. Acta* **1983**, *71*, 155.

(18) Davila, J.; Bignozzi, C. A.; Scandola, F. *J. Phys. Chem.* **1989**, *93*, 1373.

(19) (a) Giordano, P. J.; Bock, C. R.; Wrighton, M. S. *J. Am. Chem. Soc.* **1978**, *100*, 6960. (b) Giordano, P. J.; Bock, C. R.; Wrighton, M. S.; Interrant, L. V.; Williams, R. F. X. *J. Am. Chem. Soc.* **1977**, *99*, 3187.

(20) Crutchley, R. J.; Kress, N.; Lever, A. B. P. *J. Am. Chem. Soc.* **1983**, *105*, 1170.

(21) Lay, P. A.; Sasse, W. H. F. *Inorg. Chem.* **1984**, *23*, 4123.

(22) Kirsch-De Mesmaeker, A.; Jacquet, L.; Nasielski, J. *Inorg. Chem.* **1988**, *27*, 4451.

(23) (a) Peterson, S. H.; Demas, J. N. *J. Am. Chem. Soc.* **1979**, *101*, 6571. (b) Peterson, S. H.; Shepherd, R. E. *Inorg. Chem.* **1983**, *22*, 1117.

(24) Shimizu, T.; Iyoda, T.; Izaki, K. *J. Phys. Chem.* **1985**, *89*, 642.

(25) Ford, P.; Rudd, D. F. P.; Gaunder, R.; Taube, H. *J. Am. Chem. Soc.* **1968**, *90*, 1187.

(26) Crutchley, R. J.; Kress, N.; Lever, A. P. B. *J. Am. Chem. Soc.* **1983**, *105*, 1170.

(27) Kalyanasundaram, K. *Inorg. Chem.* **1989**, *28*, 4251.

(28) (a) Ireland, J. F.; Wyatt, P. A. H. *Adv. Phys. Org. Chem.* **1976**, *12*, 132. (b) Demas, J. N. *Excited State Lifetime Measurements*; Academic Press: New York, 1983; pp 59–69.

(29) Barigelletti, F.; DeCola, L.; Balzani, V.; Hage, R.; Haasnoot, J. G.; Reedijk, J.; Vos, J. G. *Inorg. Chem.* **1989**, *28*, 4344.

(30) Hage, R. Ph.D. Dissertation, Leiden University, The Netherlands, 1991.

(31) Hage, R.; Dijkhuis, A. H.; Haasnoot, J. G.; Prins, R.; Reedijk, J.; Buchanan, B. E.; Vos, J. G. *Inorg. Chem.* **1988**, *27*, 2185.

(32) Hage, R.; Haasnoot, J. G.; Stufkens, D. J.; Snoeck, T. L.; Vos, J. G.; Reedijk, J. *Inorg. Chem.* **1989**, *28*, 1413.

(33) Nieuwenhuis, H. A.; Haasnoot, J. G.; Hage, R.; Reedijk, J.; Snoeck, T. L.; Stufkens, D. J.; Vos, J. G. *Inorg. Chem.* **1991**, *30*, 48.

(34) Hage, R.; Prins, R.; Haasnoot, J. G.; Reedijk, J.; Vos, J. G. *J. Chem. Soc. Dalton Trans.* **1986**, 1389.

(35) Buchanan, B. E.; Vos, J. G.; Kaneko, M.; van der Putten, W. J. M.; Kelly, J. M.; Hage, R.; de Graaff, R. A. G.; Prins, R.; Haasnoot, J. G.; Reedijk, J. *J. Chem. Soc., Dalton Trans.* **1990**, 2425.

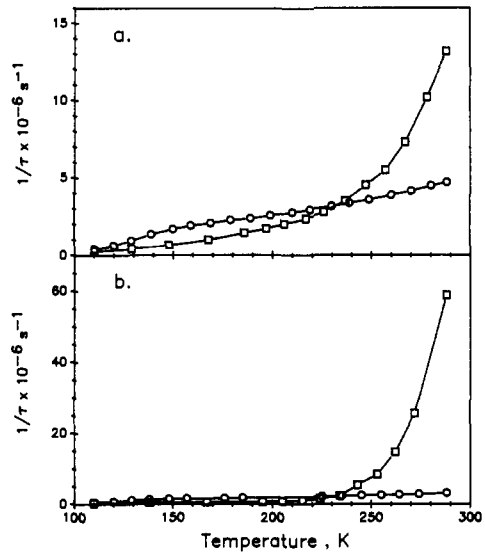

Figure 2. Luminescence decay rates of (a) $[(bpy)_2Ru(PTN\text{-}2)]^+$ (○), $[(bpy)_2Ru(HPTN\text{-}2)]^{2+}$ (□), and (b) $[(bpy)_2Ru(PTN\text{-}4)]^+$ (○), $[(bpy)_2Ru(HPTN\text{-}4)]^{2+}$ (□) as a function of temperature. The solvent in each case is 4:1 ethanol/methanol.

of both isomers when the solution pH is increased.[35] Figure 1 shows the measured luminescence lifetime and luminescence intensity of $[(bpy)_2Ru(PTN\text{-}2)]^+$ as a function of pH in buffered aqueous solutions. Luminescence decays could be fit as single exponentials at pH values greater than 3; below pH 3 the decays were fit by assuming double-exponential behavior (see Discussion and Appendix). Radiative decay rates, calculated from the observed room temperature lifetimes and quantum yields obtained at limiting high and low pH, are also given in Table I.

The temperature dependence of the luminescence lifetime of both the N-2 and N-4 isomers was examined in 4:1 ethanol/methanol solutions containing a small amount of either CF_3COOH or Et_2NH to control pH. Results over the temperature range 110–290 K are shown in Figure 2. Both isomers exhibit a much stronger temperature dependence in acidic solutions. The data were fit by assuming that the excited-state decay consists of a temperature-independent intrinsic decay from the ^{3}MLCT state and a single thermally activated nonradiative decay process (eq 1).[5] Other approaches have been used in treating tempera-

$$1/\tau_{obs} = k_0 + k' \exp(-E_a/RT) \qquad (1)$$

ture-dependent lifetimes of related Ru(II) diimine complexes; in particular, additional parameters are frequently included to fit data obtained in the solvent glass transition region (110–130 K for 4:1 ethanol/methanol).[13,29] With the exception of $[(bpy)_2Ru(PTN\text{-}2)]^+$ the data could be adequately fit without employing the solvent parameters. Results of data fit to eq 1 are given in Table II; parameters for $[(bpy)_2Ru(PTN\text{-}2)]^+$ were obtained by fitting data obtained at temperatures above the glass transition temperature (>150 K) using eq 1.

The photoreactivity of the protonated isomers was examined in CH_2Cl_2 solutions containing tetraethylammonium bromide (TEABr, 0.003 M). Both isomers are reactive and the ultimate product obtained is $[(bpy)_2RuBr_2]$. Figure 3 shows spectrophotometric changes observed upon broad band (>420 nm) photolysis of each isomer in CH_2Cl_2 containing TEABr. While $[(bpy)_2Ru(HPTN\text{-}4)]^{2+}$ maintains three isosbestic points through most of the photolysis, $[(bpy)_2Ru(HPTN\text{-}2)]^{2+}$ clearly has more than two species in solution during the photolysis. The observed loss of isosbestic behavior may result from photoinduced linkage isomerism (vide infra). In CH_2Cl_2 solutions made basic with Et_2NH (10^{-2} M), both isomers are unreactive. Even upon prolonged (>8 h) photolysis no evidence for photoanation is observed.

To examine the photoprocess of the protonated complexes in CH_2Cl_2 more carefully, aliquots taken during photolysis were examined by HPLC (Waters SCX radial compression module)

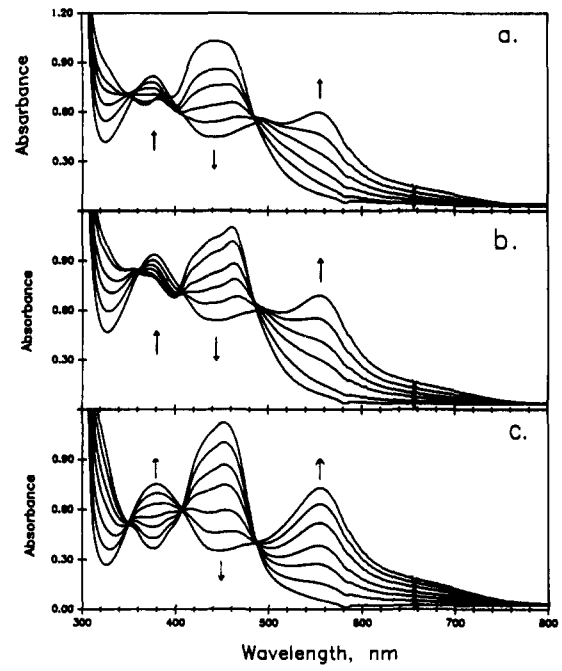

Figure 3. Room temperature spectrophotometric changes observed upon photolysis of (a) $[(bpy)_2Ru(HPTN\text{-}2)]^{2+}$, (b) $[(bpy)_2Ru(HPTN\text{-}4)]^{2+}$, and (c) $[(bpy)_3Ru]^{2+}$ in CH_2Cl_2 containing 10^{-3} M TEABr.

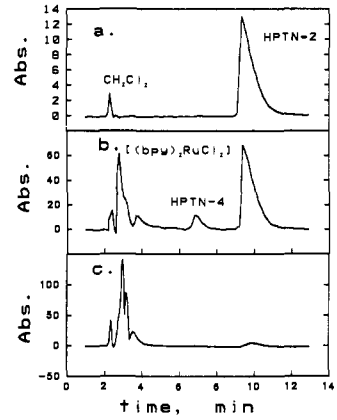

Figure 4. HPLC traces obtained upon photolysis of $[(bpy)_2Ru(HPTN\text{-}2)]^{2+}$ in CH_2Cl_2 containing 10^{-3} M TEABr at (a) 0, (b) 4, and (c) 40 min.

using diode array spectrophotometric detection. HPLC traces taken before photolysis and at two times during photolysis of $[(bpy)_2Ru(HPTN\text{-}2)]^{2+}$ are shown in Figure 4, and spectra of the fractions obtained are shown in Figure 5. Along with the free ligand and photoproduct, a second band at short retention (2.2 min) appears as an intermediate in the photolysis. The identity of the intermediate is not clear, although its spectrum (Figure 5) is similar to that of $[(bpy)_2RuBr_2]$.

Photolysis of $[(bpy)_2Ru(HPTN\text{-}2)]^{2+}$ in CH_2Cl_2 in the absence of Br^- results in partial (80%) linkage isomerism to $[(bpy)_2Ru(HPTN\text{-}4)]^{2+}$. Figure 6 shows HPLC traces obtained at several times during photolysis of the protonated complex in CH_2Cl_2. Irradiation of $[(bpy)_2Ru(HPTN\text{-}4)]^{2+}$ under the same conditions results in the formation of a small amount of $[(bpy)_2Ru(HPTN\text{-}2)]^{2+}$, observable by HPLC.

Discussion

Excited-State Acid–Base Equilibration. The protonation equilibria of excited states of numerous substances has been examined in detail, and excellent reviews of the kinetic and thermodynamic considerations exist.[28] The processes shown in Scheme I represent a simplified description of the behavior of the HPTN complexes. The scheme assumes unit efficiency for forming the ^{3}MLCT state of $[L_nML']^*$ and $[L_nML'H]^*$ and, thus, protona-

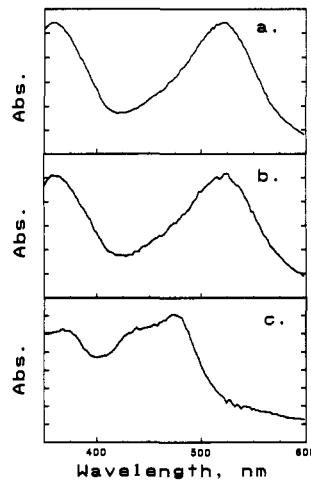

Figure 5. Absorption spectra obtained for HPLC fractions at retention times of 2.8, 3.2, and 9.4 min following room temperature photolysis of $[(bpy)_2Ru(HPTN\text{-}2)]^{2+}$ in CH_2Cl_2 containing 10^{-3} M TEABr.

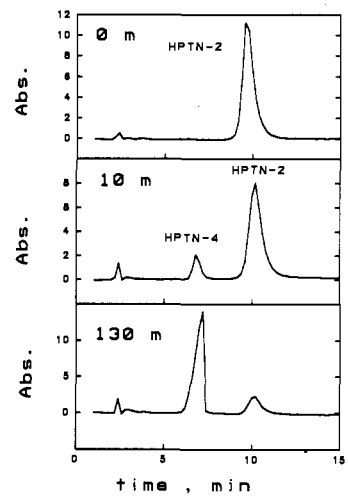

Figure 6. HPLC changes observed during photolysis of $[(bpy)_2Ru(HPTN\text{-}2)]^{2+}$ in CH_2Cl_2. Peak at early times (t < 2 min) is CH_2Cl_2.

tion/deprotonation is not important in the singlet MLCT state. The scheme also assumes that protonation does not quench the excited state of either form of the complex. With the above assumptions, the excited-state pK values (pK_{ae}) of $[(bpy)_2Ru(HPTN\text{-}2)]^{2+}$ and $[(bpy)_2Ru(HPTN\text{-}4)]^{2+}$ can be determined from both steady-state and time-resolved luminescence measurements. The pK_{ae} can be determined from Förster cycle analysis[28] of Scheme I if the energy gap between the zeroth vibrational levels of the ground and excited states can be determined and the pK_{ag} of the ground state is known (eq 2). In the

$$pK_{ae} = pK_{ag} + (0.625/T)[E_\infty^b - E_\infty^a] \quad (cm^{-1}) \qquad (2)$$

equation E_∞^b and E_∞^a are the energy gaps for the PTN and HPTN complexes, respectively.[28,35] Acid dissociation values for the excited complexes determined by eq 2 are given in Table III. The values of Table III were determined using room temperature luminescence maxima in Britton–Robinson buffer rather than E_∞ values.[37]

The excited-state pK_{ae} value can also be determined from the inflection point of the luminescence intensity vs pH titration curve. pK_{ae} values determined in this manner require the further assumption that the luminescence lifetimes of the protonated and free base forms are identical, which is clearly not the case here. To correct for differences in the lifetimes of the two forms, eq 3 has been used, where pH_i is the inflection point of the luminescence intensity titration curve and τ_a and τ_b are the lifetimes of the protonated and basic forms of the complex, respectively (Table III).[28,35] An assumption of eq 3 is that the rate constant for protonation of $[L_nML']^*$ is larger than the decay rate constant for the deprotonated complex, k_{nr}, and the dissociation rate constant of $[L_nML'H]^*$ is greater than k_{nrH}. For both $[(bpy)_2Ru(HPTN)]^{2+}$ complexes the lifetime is less than 10 ns. The rate of deprotonation can be estimated from the pK_{ae} ($K_{ae} = k_{-H}/k_H$) values obtained from the Förster cycle. If it is assumed that the protonation is diffusion limited, k_H will be approximately 10^{10} M^{-1} s^{-1}. Given these approximations k_{-H} will be 6×10^7 s^{-1} for $[(bpy)_2Ru(HPTN\text{-}2)]^{2+}$ and 6×10^5 s^{-1} for $[(bpy)_2Ru(HPTN\text{-}4)]^{2+}$. The inference is that both the HPTN-2 and HPTN-4 complexes are very likely *not* equilibrated in the excited state.

$$pK_{ae} = pH_i + \log(\tau_a/\tau_b) \qquad (3)$$

Table III. Ground- and Excited-State pK Values of $[(bpy)_2Ru(HPTN\text{-}2)]^{2+}$ and $[(bpy)_2Ru(HPTN\text{-}4)]^{2+}$

complex	pK_{ag}[a]	pK_{ae}[a]	pH_i[b]	p$K_{ae}(\tau)$[b]
HPTN-2	4.07	2.2	2.8	1.4
HPTN-4	5.7	4.2	5.1	3.1

[a] From ref 35. [b] pH_i = inflection point of emission intensity titration; p$K_{ae}(\tau)$ calculated using eq 3.

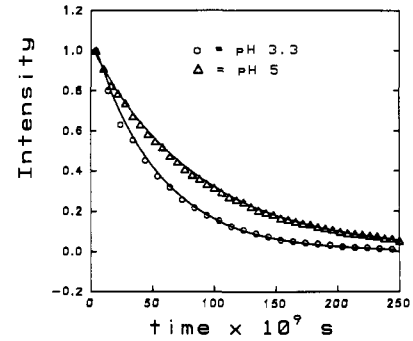

Figure 7. Excited-state decay of $[(bpy)_2Ru(PTN\text{-}2)]^+$ in Britton–Robinson buffer at pH 5 and 3.3 at 298 K. Solid lines represent fits to the data using eq A1 of the Appendix assuming $k_{nr} = 1.1 \times 10^7$ s^{-1}, $k_{nrH} = 5 \times 10^8$ s^{-1}, p$K_{ag} = 4.07$, p$K_{ae} = 2.1$, and $k_H = 3 \times 10^{10}$ M^{-1} s^{-1}.

Excited-State Decay in Acid and Base. Both the HPTN-2 and HPTN-4 complexes exhibit single-exponential decay behavior over a wide pH range in aqueous buffer solutions. Scheme I is adequate to describe the excited-state decay behavior of the complexes, and the general solution for the excited-state decay of both protonated and deprotonated complexes is given in the Appendix. By assuming the observed luminescence decays at very high and very low pH represent decays for pure $[(bpy)_2Ru(PTN\text{-}2)]^+$ and $[(bpy)_2Ru(HPTN\text{-}2)]^{2+}$, the pH-dependent luminescence decays can be fit with only K_{ae} and k_H as variable parameters. Figure 7 shows experimental and calculated decays (using eq A1 of the Appendix) for $[(bpy)_2Ru(PTN\text{-}2)]^+$ at pH 5 and 3.3. Decays at pH values where both protonated and deprotonated complexes are present should be double exponential since both complexes luminesce at the wavelength used for data acquisition (650 nm). However, the decay of the protonated complex is rapid enough that simultaneous observation of both decays was not possible with the apparatus used. Thus, the fit assumes observation of only the deprotonated complex. The calculated decay curves are very sensitive to the value of k_H, and reasonable fits to the observed decays are only obtained when k_H is greater than 10^{10} M^{-1} s^{-1}. The significance of the large k_H is that protonation effectively becomes a nonradiative decay path of $[(bpy)_2Ru(PTN\text{-}2)]^+$ since decay of the excited protonated complex is also very fast ($k_{nrH} = 5 \times 10^8$ s^{-1}). Also, reasonable fits were obtained only when pK_{ae} was between 2.0 and 2.2; steady-state emission titration

(36) (a) Caspar, J. V.; Meyer, T. J. *Inorg. Chem.* **1983**, *22*, 2444. (b) Caspar, J. V.; Meyer, T. J. *J. Am. Chem. Soc.* **1983**, *105*, 5583.

(37) The luminescence maximum does not reflect the true $v_0 - v_0(E_\infty)$ energy gap between the ground state and ^{3}MLCT state. A more precise measure of E_∞ can be obtained by fitting the luminescence spectrum using a model having a single promoting and accepting mode for nonradiative relaxation.[4,36] The approximation of using maxima assumes the absorption and luminescence bands have the same bandwidth.

estimates of pK_{ae} yielded lower values (Table III) for the HPTN-2 complex (eq 3). An approximation of eq 3 is that k_{-H} is greater than k_{nrH}; constants obtained from fits of emission decays (Figure 7) indicate that the protonation rate constant is actually lower than k_{nrH}, suggesting the pK_{ae} value obtained by eq 3 is invalid. Finally, Förster cycle estimates of pK_{ae} compare favorably with those estimated from fits of pH-dependent luminescence decays.

Temperature-Dependent Lifetimes. The origin of the much shorter luminescence lifetime of the protonated complexes relative to that of the deprotonated complexes is not clear. In many Ru(II) diimine complexes, a competing path for nonradiative relaxation is the thermally activated population of a ^{3}MC state close in energy to the ^{3}MLCT state (vide supra). In studies of effects of protonation on the excited-state behavior of $[(bpy)_2Ru(CN)_2]$, Scandola and co-workers postulated that protonation of the complex results in a decrease in the ^{3}MLCT–^{3}MC gap and a subsequent increase in the nonradiative relaxation rate.[18] In the case of the pyridyltriazole complexes, protonation results in an increase in the emission energy. The MLCT transition results from a $Ru(d\pi) \rightarrow bpy(\pi^*)$ transition, while the MC state has as its origin a $Ru(d\pi) \rightarrow Ru(e_g^*)$ transition.[1-4] Protonation of the complex results in stabilization of the ground state since HPTN is a better π-accepting ligand than PTN. Further, HPTN is a weaker σ-donating ligand than PTN and, assuming an averaged ligand field environment for both protonated and deprotonated complexes, the $Ru(d\pi) \rightarrow Ru(e_g^*)$ energy should be larger for the deprotonated complex. Thus, both changes in metal–ligand interaction which occur upon protonation should serve to decrease the energy gap between the ^{3}MLCT and ^{3}MC states, and it is reasonable that the decrease in the luminescence lifetime upon protonation of the PTN complexes may result from facile internal conversion to a ^{3}MC state which rapidly relaxes to the ground state.

The ^{3}MC-state energies cannot be determined directly, but the gap between ^{3}MLCT and ^{3}MC states can be approximated from activation parameters obtained from temperature-dependent luminescence lifetimes.[9b] Activation parameters obtained for ^{3}MLCT emission of complexes usually fall into one of two categories: (a) small activation energies (<800 cm^{-1}) and low prefactors ($<10^9$ s^{-1}) or (b) large activation energies (>2000 cm^{-1}) and large prefactors ($>10^{11}$ s^{-1}).[1,4,18] In the second case the activated process has been ascribed to population of the ^{3}MC state. If relaxation of the ^{3}MC state is rapid relative to crossover from the ^{3}MC state back to the ^{3}MLCT state, the measured E_a represents the activation energy for ^{3}MLCT–^{3}MC internal conversion (case b1). Since the process is viewed as an electron transfer in a strongly coupled system, the prefactor is expected to be large (10^{13}–10^{14}). If the ^{3}MLCT and ^{3}MC states are in equilibrium, the measured activation energy corresponds approximately to the energy gap between the two states (case b2).[9b] In this case the prefactor for the process will generally be lower than that for the case of rapid ^{3}MC-state decay (10^{10}–10^{12} s^{-1}).

When both the activation barrier and prefactor are small, case a, interpretation of the data is less clear. Complexes exhibiting this behavior are typically unreactive to photosubstitution and, as a result, it is unlikely population of a ^{3}MC state occurs.[7,9,12,13] The low prefactor also suggests the process involves population of a state only weakly coupled to the ^{3}MLCT state. On the basis of these observations and molecular orbital calculations, Kober and Meyer have postulated that this activated process corresponds to population of a MLCT state of largely singlet character.[4,38]

From the activation parameters obtained for the two isomers in both acidic and basic ethanol/methanol (4:1), it appears that only the protonated complexes have prefactors and activation barriers common to complexes having an accessible ^{3}MC state. The deprotonated forms of both complexes have low prefactors and small activation barriers characteristic of photoinert complexes (case a). $[(bpy)_2Ru(HPTN\text{-}2)]^{2+}$ exhibits intermediate behavior; however, the prefactor of 6×10^{10} s^{-1} and the 1700-cm^{-1} "activation" barrier are not unreasonable for ^{3}MLCT and ^{3}MC states in equilibrium (case b2).[1-4] The activation parameters obtained in this manner can be used to estimate the efficiency for population of the ^{3}MC state (eq 4). Values calculated for

$$\eta_{ic} = k' \exp(-E_a/RT)/(k_0 + k' \exp(-E_a/RT)) \quad (4)$$

both the protonated complexes using k' and E_a obtained from temperature-dependent luminescence lifetimes are given in Table II. In each case the estimated internal conversion efficiency is high (>0.9).

Photoanation and Photoinduced Linkage Isomerism. One measure of the validity of the above explanation for excited-state decay is the susceptibility of the complexes to photoanation in nonpolar solvents. For $[(bpy)_3Ru]^{2+}$ and numerous other tris-(diimine) complexes, photolysis in the presence of halide results in clean conversion of the tris complex to the bis halo complex (eq 5). This photoanation process does not occur readily for

$$[Ru(L)_3]^{2+} + 2X^- \xrightarrow[CH_2Cl_2]{h\nu} [Ru(L)_2X_2] + L \quad (5)$$

complexes having ^{3}MC states which are not accessible from the ^{3}MCLT state.[9b,12,13] As shown in Figure 3, photolysis of either $[(bpy)_2Ru(HPTN\text{-}4)]^{2+}$ or $[(bpy)_2Ru(HPTN\text{-}2)]^{2+}$ in CH_2Cl_2 containing Br^- results in the formation of a *cis*-Br^- complex. Neither deprotonated complex is photolabile in CH_2Cl_2 solutions containing Br^- and base. Thus, the photoreactivity of the complexes is consistent with the excited-state decay behavior discussed above; only complexes having a high efficiency for population of the ^{3}MC state (Table II) exhibit photolability. The result is that the photoreactivity of these complexes can be controlled simply by adjusting the pH of the environment.

In a related study, the photoanation behavior of $[(bpy)_2Ru(bpt)]^+$ (bpt = 3,5-bis(pyridin-2-yl)-1,2,4-triazolate ion) and the dinuclear complex $\{[(bpy)_2Ru]_2bpt\}^{3+}$ was recently reported by Barigelletti and co-workers.[29] The mononuclear complex is photoinert and has activation parameters for nonradiative decay similar to those of $[(bpy)_2Ru(PTN\text{-}2)]^+$ ($k' = 6.5 \times 10^7$ s^{-1} and $E_a = 660$ cm^{-1} in 4:5 propionitrile/butyronitrile). The dinuclear complex exhibits photophysical characteristics and photoanation behavior similar to those of $[(bpy)_2Ru(HPTN\text{-}2)]^{2+}$. The photoreactivity of $\{[(bpy)_2Ru]_2bpt\}^{3+}$ was attributed to population of a ^{3}MC state made accessible because the ligand field strength of the bpt ligand decreases upon coordination to the second metal center (analogous to protonation). The same behavior is observed upon protonation of the coordinated PTN ligands.

Figure 3 also shows that isosbestic points are not observed in the photolysis of the protonated form of the complexes, indicating the presence of species other than the starting material and product in solution. HPLC analysis of solutions of $[(bpy)_2Ru(HPTN\text{-}2)]^{2+}$ during photolysis reveals the presence of $[(bpy)_2Ru(HPTN\text{-}4)]^{2+}$ ($t_r \sim 7$ min, Figure 4). The observation suggests that a monodentate form of the pyridyltriazole complex is formed during photolysis which either anneals to starting complex, undergoes linkage isomerism to form $[(bpy)_2Ru(HPTN\text{-}4)]^{2+}$, or halogenates to form a monodentate intermediate which goes on to form product. Scheme II illustrates the chemistry of the ^{3}MC state of $[(bpy)_2Ru(HPTN\text{-}2)]^{2+}$ in solutions containing halide. The scheme suggests that linkage isomerism of the protonated form of either complex should occur upon photolysis in the absence of halide. Figure 6 illustrates HPLC changes observed upon photolysis of $[(bpy)_2Ru(HPTN\text{-}2)]^{2+}$ in CH_2Cl_2. The new band observed corresponds to formation of $[(bpy)_2Ru(HPTN\text{-}4)]^{2+}$; equilibrium is reached at 4:1 $[(bpy)_2Ru(HPTN\text{-}4)]^{2+}$/$[(bpy)_2Ru(HPTN\text{-}2)]^{2+}$. The relative basicities of the noncoordinated nitrogens of $[(bpy)_2Ru(PTN\text{-}2)]^{2+}$ ($pK = 4.07$) and $[(bpy)_2Ru(PTN\text{-}4)]^{2+}$ ($pK = 5.7$) indicate that the free nitrogen of PTN-2 (N-4) is a weaker base than that of PTN-4 (N-2). If this remains true for the monodentate intermediate of Scheme II, the predominant form will have N-2 protonated and N-4 can coordinate. It is also possible that the observed steady state reflects differing efficiencies for forming monodentate intermediates from the ^{3}MC state of the N-2 and N-4 bound complexes (the data of Table II indicate the efficiency of forming the ^{3}MC state is

(38) Kober, E. M.; Meyer, T. J. *Inorg. Chem.* **1984**, *23*, 3877.

Scheme II

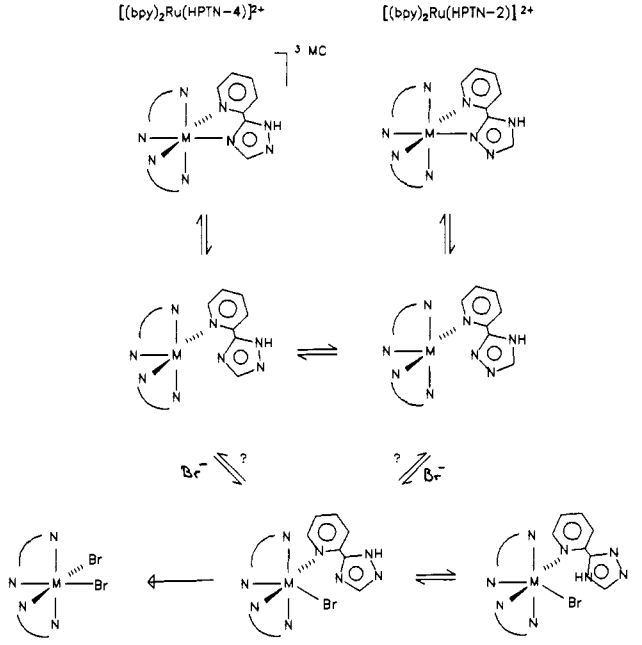

nearly the same for the two complexes). The photoinduced linkage isomerism is also consistent with the observed labilization of the pyridyltriazole to yield $[(bpy)_2RuBr_2]$ as the final photolysis product.

One aspect of the photoanation that remains unclear is the identity of the intermediate species observed at short retention times in HPLC (Figures 4 and 5). The intermediate is not likely to represent the monobromo complex, since related monobromo complexes have MLCT absorption maxima around 500 nm. The low retention time on the cation-exchange column suggests the complex is uncharged. We are currently investigating this in more detail.

Summary. Protonation of both linkage isomers of $[(bpy)_2Ru(PTN)]^+$ results in a decrease in the luminescence lifetime in solution and an increase in reactivity upon photolysis in CH_2Cl_2. Results of temperature-dependent luminescence decays suggest the protonated complexes decay via population of a ^3MC state, while the deprotonated complexes do not efficiently populate this state at or below room temperature. Photolysis of either protonated isomer in CH_2Cl_2 results in linkage isomerism; equilibrium is established at 4:1 $[(bpy)_2Ru(PTN\text{-}4)]^{2+}/[(bpy)_2Ru(PTN\text{-}2)]^{2+}$. In the presence of a coordinating counterion, photoanation occurs to yield the cis-anion complex with loss of pyridyltriazole. The basic form of both isomers is inert to photosubstitution in CH_2Cl_2 at room temperature. Thus, the substitutional photolability can be controlled by controlling protonation of the ground state of the complex.

Experimental Section

Materials. The synthesis, semiprepartive HPLC separation, and characterization of the two isomers of $[(bpy)_2Ru(HPTN)](PF_6)_2$ have been described in previous work.[17c,34,35] $[(bpy)_3Ru](PF_6)_2$ was prepared according to a literature method.[39]

Britton–Robinson buffer (a mixture of 0.04 M acetic acid, phosphoric acid, and boric acid) was made using deionized water. All of the other solvents (EM Science) were used without further purification.

pH-Dependent Lifetime Measurements. The samples were dissolved in ca. 20 mL of CH_3CN and then added to 150 mL of Britton–Robinson buffer. The pH was adjusted by addition of H_2SO_4 or NaOH and measured with an EXTECH 651 digital pH meter.

Luminescence lifetimes were measured by direct transient digitization of luminescence decays using a modification of apparatus described earlier.[9b] The excitation source was a Laser Photonics LN1000 Mega-Plus nitrogen laser, (wavelength 337 nm, pulse width 600 ps). Emitted light from the sample was collected at right angles to the incident excitation beam. Corning glass cutoff filters were used to remove scattered laser light, and the emitted light was imaged onto the entrance slit of a GCA/McPherson EU-700 monochromotor (λ = 650 nm) and detected with a Hamamatsu R777 PMT in a Pacific Instruments 3150 PF holder. The PMT output was captured using a HP54111D digitizer (limited to 8-bit vertical resolution). Triggering was accomplished by splitting off a fraction of laser beam to saturate a photodiode. Experiments were controlled by a Hewlett-Packard 9826 microcomputer interfaced to a HP 6940 B multiprogrammer. Lifetime data were analyzed by using a nonlinear least-squares fit to exponential decay. The fitting program uses a modified Marquardt algorithm for least-squares minimizations.[40]

For samples having pH <1.7, the lifetime data were recorded on a time-correlated single photon counting system employing a mode locked, cavity dumped Ar^+ laser for excitation (doubled dye output at 295 nm).[41]

Variable-temperature luminescence lifetime measurements were made using an Air Products Displex cryostat. Sealed samples in 2-mm × 3-cm cylindrical tubes were placed in a home-built copper sample holder and mounted to the cryostat. Samples were prepared by dissolving the solid in 4:1 EtOH/MeOH. Ten microliters of either Et_2NH or CF_3COOH was added to 5-mL sample solutions to ensure deprotonation/protonation. The solutions were freeze–pump–thaw degassed for at least six cycles and sealed under vacuum. Temperatures were measured at the tip of the cryostate; samples were equilibrated for 20 min at each temperature.

Photolyses. a. Photolysis in $TEAB/CH_2Cl_2$ Monitored by UV–vis Absorption Spectroscopy. Solutions for photolysis of the protonated complexes were prepared by mixing equal volumes of the protonated complex in CH_2Cl_2 ($\simeq 10^{-5}$ M) and tetraethylammonium bromide (6.0×10^{-3} M) in a 1-cm Pyrex fluorometric cell. In the case of deprotonated samples, 10 μL of Et_2NH was added to solutions prepared as above. All of the preparations were performed in the dark, and all solutions were deaerated by bubbling with solvent-saturated N_2 for 15 min. Absorption spectra were measured as a function of time during photolysis by using a Hewlett-Packard 8451A diode array spectrophotometer. The N_2 bubble degassed sample solutions in sealed Pyrex glass cells were mounted in a fixed position using a Model EU-701-11 Heath sample cell module. Photolysis light (Ealing 250 W universal broad band Xe arc lamp) was focused onto the glass window of the cell module, and UV and infrared frequencies were filtered by using Schott GG 400 and Corning 4-71 glass filters and passing the excitation through a water bath (5-cm path).

b. Photolysis in CH_2Cl_2 or $TEAB/CH_2Cl_2$ Monitored by HPLC. The preparation of solutions for photolyses in $TEAB/CH_2Cl_2$ and the apparatus are the same as described above. High-performance liquid chromatography was carried out with a Waters HPLC system which includes a 990 photodiode array detector, a Waters Model 6000A pump, a 20 μL injector loop, and a 10 Partisil SCX 8-mm × 10-cm cation-exchange column mounted in a Waters radial compression Z module. All of the separations were controlled by a PAC III computer. Chromatograms were monitored at 280 nm. The volume of the solution injected each time was 20 μL. The mobile phase was (80:20) $CH_3CN:H_2O$ containing 0.08 M $LiClO_4$. Flow rates used were 2.5 mL/min. The photolysis of the two isomers in CH_2Cl_2 only (in the absence of TEAB or base) was carried out in the same way as described above.

Emission and Photoanation Quantum Yields. Room temperature quantum yields were measured by using a Spex Industries Model III C fluorescence spectrometer equipped with a 450-W Xe arc lamp, cooled PMT housing and thermostated cell holder.

The samples were dissolved in CH_3CN and ca. 10 μL CF_3COOH or Et_2NH was added into 5 mL of solution to confirm protonation/deprotonation. The absorbance of all the solutions was matched at 0.5 ODU at the excitation wavelength (440 nm). The solutions were degassed with bubbled nitrogen for 30 min prior to measurements, and a blanket of N_2 was maintained during the measurements. Emission measurements were made at 90° relative to excitation, and the data were not corrected for photomultiplier response. Quantum yields for the two isomers were calculated from the integrated emission spectra relative to $[(bpy)_3]Ru^{2+}$ in CH_3CN (Φ_r = 0.062).[39]

Photoanation quantum yields were measured using the same solutions for photolysis in $TEAB/CH_2Cl_2$ while the absorbance at excitation wavelength (468 nm) was adjusted to be matched at $\simeq$0.40 ODU. The solutions were deaerated by N_2 purging for 30 min. The photoanation was monitored by measuring the emission intensity at 650 nm as a function of time. The emission intensity decreased linearly near the beginning of the photolysis (typically <100 s, only <10% conversion to product), and the ratios of the slopes calculated from the linear regression

(39) Calvert, J. M.; Casper, J. V.; Binstead, R. A.; Westmoreland, T. D.; Meyer, T. J. *J. Am. Chem. Soc.* **1982**, *104*, 6620.

(40) Marquardt, D. W. *Soc. Ind. Appl. Math.* **1963**, *11*, 431.

(41) Sipior, J.; Sulkes, M.; Auerbach, R. A.; Boivineau, M. *J. Phys. Chem.* **1987**, *91*, 2016.

data were used to determine the photoanation quantum yields relative to $[(bpy)_3Ru]^{2+}$.

Acknowledgment. R.H.S. thanks the Louisiana Educational Quality Support Fund, administered by the Louisiana State Board of Regents, for support of this work. We acknowledge financial support from EOLAS, the Irish Science and Technology Agency. We also thank Johnson Matthey for a generous load of ruthenium trichloride.

Appendix

Ireland and Wyatt[28] and others have stated the general solution for luminescence decay of protonated and deprotonated species in equilibrium (Scheme I). The solution for particular cases requires knowledge of five constants: the ground-state acid dissociation constant (K_{ag}), the decay rate constants of the protonated (k_{nrH}) and deprotonated (k_{nr}) complexes, and the rate constants for protonation (k_H) and deprotonation (k_{-H}) of the excited complex. By assuming both the protonated (HPTN) and deprotonated (PTN) complexes have the same molar absorptivity at the excitation wavelength (λ = 337 nm),[35] the fractions, f, of PTN and HPTN in solution immediately following excitation at any given pH can be determined from K_{ag}:

$$[PTN]_T = [HPTN]_0 + [PTN]_0$$

$$f^0_{HPTN} = [HPTN]_0/[PTN]_T = [H^+]/(K_{ag} + [H^+])$$

$$f^0_{PTN} = [PTN]_0/[PTN]_T = 1 - [HPTN]_0$$

The concentration of excited PTN and HPTN at any time following excitation can be written from the general expression of Ireland and Wyatt (see Scheme I):[28]

$$\frac{[PTN]_t}{[PTN]_T} = \frac{1}{2\lambda}\{[(\lambda - k_p + k_d)f^0_{PTN} - 2k_{-H}f^0_{HPTN}]\exp(-\alpha t) + [(\lambda + k_p - k_d)f^0_{PTN} + 2k_{-H}f^0_{HPTN}]\exp(-\beta t)\} \quad (A1)$$

$$\frac{[HPTN]_t}{[PTN]_T} = \frac{1}{2\lambda}\{[(\lambda + k_p - k_d)f^0_{HPTN} - 2k_H[H^+]f^0_{PTN}] \times \exp(-\alpha t) + [(\lambda - k_p + k_d)f^0_{HPTN} + 2k_H[H^+]f^0_{PTN}]\exp(-\beta t)\} \quad (A2)$$

$$\lambda = \sqrt{(k_p - k_d)^2 + 4k_{-H}k_H[H^+]}$$

$$\alpha = (k_p + k_d + \lambda)/2$$

$$\beta = (k_p + k_d - \lambda)/2$$

$$k_p = k_{nrH} + k_{-H} \qquad k_d = k_{nr} + k_H[H^+]$$

Since decay of the protonated complex is very fast ($k_{nrH} \sim 2$-5×10^8 s^{-1}), it is assumed that the predominant emitting species in solution at times >10 ns is the deprotonated complex. Data were fit to eq A1 by using experimental values of K_{ag}, k_{nrH}, and k_{nr}, assuming a value of K_{ae}, and having a single variable parameter, k_H ($k_{-H} = K_{ae}k_H$). Figure 7 illustrates results obtained using this fitting procedure.

Time-Resolved Charge-Transfer Spectroscopy of Aromatic EDA Complexes with Nitrosonium. Inner-Sphere Mechanism for Electron Transfer in the Isoergonic Region

T. M. Bockman, Z. J. Karpinski, S. Sankararaman, and J. K. Kochi*

Contribution from the Chemistry Department, University of Houston, Houston, Texas 77204-5641. *Received December 17, 1990. Revised Manuscript Received October 29, 1991*

Abstract: Photoinduced electron transfer in various 1:1 aromatic EDA complexes with nitrosonium by the direct laser-pulse (20-ps and 10-ns fwhm) excitation of the charge-transfer bands leads to the spontaneous generation of the redox pair $Ar^{\bullet+}$ and NO. Temporal relaxation by back electron transfer to regenerate the EDA complex $[Ar,NO^+]$ is measured by following the spectral decay of $Ar^{\bullet+}$ with the aid of time-resolved spectroscopy over the two separate time domains I and II. *Picosecond kinetics* (k_I) are associated with the first-order collapse of the geminate ion radical $[Ar^{\bullet+},NO]$ by inner-sphere electron transfer back to the EDA complex—the relatively slow rates with $k_I \sim 10^8$ s^{-1} arising from driving forces that approach the isoergonic region, coupled with the rather high reorganization energy of nitric oxide. These allow effective competition from diffusive separation (k_s) to form $Ar^{\bullet+}$ and NO as kinetically separate entities. *Microsecond kinetics* (k_{II}) are thus associated with the second-order (back) electron transfer from the freely diffusing $Ar^{\bullet+}$ and NO. However, the comparison of the second-order rate constants calculated from Marcus theory shows that outer-sphere electron transfer is too slow to account for the experimental values of k_{II}. The second-order process is unambiguously identified (by the use of the thermochemical cycle in Scheme IV) as the alternative, more circuitous inner-sphere pathway involving the (re)association (k_a) of $Ar^{\bullet+}$ and NO to afford the cation radical pair $[Ar^{\bullet+},NO]$ followed by its collapse to the EDA complex. The general implications of inner-sphere complexes as reactive intermediates in electron transfer mechanisms in the isoergonic and endergonic regions are presented.

Introduction

The nitrosonium ion NO^+ is an unusually versatile species—a simple diatomic cation that is coordinatively unsaturated, easily formed, and uncommonly persistent in solution.[1] Being isoelectronic with carbon monoxide, NO^+ is an excellent ligand;[2] but it has also been used as an active electrophile[3] as well as an effective oxidant[4] in electron-transfer processes due to its rather

(1) Cotton, F. A.; Wilkinson, G. *Advanced Inorganic Chemistry*; 5th ed.; Wiley: New York, 1988; p 321 ff.

(2) (a) McCleverty, J. A. *Chem. Rev.* **1979**, *79*, 53. (b) Feltham, R. D.; Enemark, J. H. In *Topics in Inorganic and Organometallic Stereochemistry*; Geoffroy, G., Ed.; Wiley: New York, 1981. (c) Pandey, K. K. *Coord. Chem. Rev.* **1983**, *51*, 69. (d) Hawkins, T. W.; Hall, M. B. *Inorg. Chem.* **1980**, *19*, 1735. (e) Enemark, J. H.; Feltham, R. D. *Coord. Chem. Rev.* **1974**, *13*, 339. (f) Connelly, N. G. *Inorg. Chim. Acta Rev.* **1972**, *6*, 47. (g) Frenz, B. A.; Ibers, J. A. *M. T. P. Int. Rev. Sci. Phys. Chem. Ser. One* **1972**, *11*, 33. (h) Griffith, W. P. *Adv. Organomet. Chem.* **1968**, *7*, 211.

0002-7863/92/1514-1970$03.00/0